Iranian Journal of Mathematical Sciences and Informatics
Vol. 20, No. 1 (2025), pp 53-67
DOI: 10.61186/ijmsi.20.1.53

Image Enhancement and Restoration Approach Based on Anisotropic Diffusion

Messaouda Gatcha[a], Farid Messelmi[b*], Slami Saadi[a]

[a]Faculty of Exact Sciences and Computers, Applied Automation and Industrial Diagnosis Laboratory, Ziane Achour University, Djelfa, Algeria
[b]Faculty of Exact Sciences and Computers, Development in Mechanics and Materials Laboratory, Ziane Achour University, Djelfa, Algeria

E-mail: messaoudamath2017@gmail.com
E-mail: foudimath@yahoo.fr
E-mail: saadisdz@gmail.com

Abstract. We propose a new approach for image enhancement, denoising and restoration, using an anisotropic diffusion based on P-M model and L.V and al. equation, replacing the gradient by motion by mean curvature to detect noise direction for each degraded pixel locally, applying the gradient in Gaussian kernel term to restore the degraded pixels and adding a time term supporting the restoration process. For execution progress, the numerical discretization for the terms of PDE modeling (obtained by the approximation by difference finite volumes finite method, Taylor method and Simpsons improved method), concludes an algorithm treats noised image regardless the noise type (salt-pepper or Gaussian or speckle) better than other filters based whether on anisotropic diffusion or total, shown in the experimental results (using MATLAB program), and demonstrated through PSNR and SSIM.

Keywords: Image restoration, Anisotropic diffusion, Regularization, Noise filters.
2020 Mathematics subject classification: 94A08, 68R99, 68U10.

*Corresponding Author

Received 07 December 2019; Accepted 10 March 2025
©2025 Academic Center for Education, Culture and Research TMU

1. Introduction

Image restoration (denoising, smoothing, enhancing...) stills an important field of image processing with the expanding of computerized treatment and intelligent artificial vision. As seen, we live in vision era (HD, QLED, 4K, Holographic...), when the latest capture devices and sensor machines seek the high definition through the manipulation of image to reach more realistic focus, consequently poor image quality is less present but yet there are noised or blurred ones. Looking for mathematical modeling to restore and enhance degraded images starts with edges detector by Marr-Hildreth [11]by finding the zero-crossing of the second derivative D^2 of intensity

$$f(x,y) = D^2 \left[G(r) * I(x,y)\right].$$

Taken the direction coincides with the orientation formed locally by its zero-crossing, then J. J. Koenderink [9] runs into the image structure using the divergence of image focusing on blurred ones, Perona-Malik [13] motivates enormous approaches against total variation regularization. The robust of P-M equation is the anisotropic diffusion, which models the edge as a step function convolved with Gaussian

$$I_t = div\left(c(t,x,y)\,.\nabla I\right).$$

Two years later by L. Alvarez and al.[1], motion by mean curvature appears in the degenerate diffusion term which diffuses image I in the orthogonal direction to its gradient DI and does not diffuse at all in the direction of DI thru a PDE system as

$$\begin{cases} I_t = g\left(|G * DI|\right).\left|DI\right|.div\left(\frac{DI}{|DI|}\right) \\ I(0,x,y) = I_0(x,y). \end{cases}$$

2. New approach proposed for image restoration

2.1. **System description.** The image in gray level; adapted by electronic device; mathematically is two dimension differentiable function I from open subset Ω of $\mathbb{R}^2$ to $\mathbb{R}$, while digitally is a matrix of pixels with integer values between 0 (black) and 255(white).

$$I : (a,b) \times (a',b') \subset \mathbb{R}^2 \longrightarrow \mathbb{R}.$$

I is the image in gray level, $dim(I) = 2$; $(a,b) \times (a',b') = size(I)$.
Where (a,b) is image width and (a',b') is image length.
$I(x,y)$ is the pixel for (x,y) position where $x \in (a,b)$ its horizontal position and $y \in (a',b')$ its vertical position.

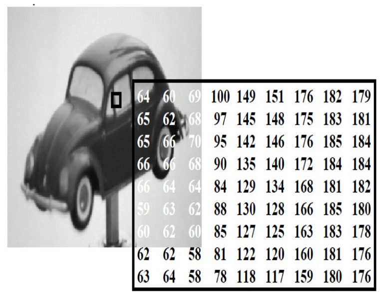

FIGURE 1. Image in gray level and part of its pixels values.

The noise mask changes in image some pixels from original values to another ones like into 0 and 255 used in salt-pepper noise. So, for that, the problem posed in noised image is ill-posed, because we don't know the type of noise, so the convenient denoising filter to rid of is also unknown; we have to estimate the degraded pixel then dispose it and research an assessment of its original value, usually through the neighboring pixels.

	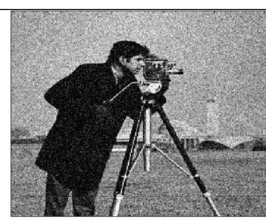	
FIGURE 2. Original image.	FIGURE 3. Noised image by salt-Pepper noise.	FIGURE 4. Noised image by additive Gaussian noise.

Our anisotropic diffusion approach[6] is on the basis of PDE contains motion by mean curvature,convolution product and Gaussian kernel and the diffusion problem coefficient term.

$$\begin{cases} I_t = c(t).\left|\nabla G_\sigma * I\right|.\left|\nabla I\right|.div\left(\frac{\nabla I}{|\nabla I|}\right) \\ I(0,x,y) = I_0(x,y) \end{cases} \tag{1.1}$$

considering that

- I_0 the noised image to start with, I_t the image obtained at the moment t during the execution process.

- The diffusion problem coefficient term $c(t) = 1 + \frac{1}{\sqrt{4+t^2}}$ helps to enhance the image contrast and keeps it from turning darker during the execution process.
- The motion by mean curvature term is degenerated diffusion term $|\nabla I| .div \left(\frac{\nabla I}{|\nabla I|}\right)$ precises the noised pixel and noise direction in its multi direction neighboring.
- $|\nabla G_\sigma * I|$ Gaussian kernel mask with σ standard deviation for noised pixel restoration with $\sigma \times \sigma$ mask rang, since there is strong association between noised pixel and its neighboring ones, therefore we can identify the original value for degraded pixel.

The analytic solution for PDE is hard to find, as usual, we are going to solve it numerically by finite differences FD method [7]; Simpsons improved method [7] and the convolution product[3, 4]. Unlike the usual, for the numerical methods where it needs the step **h** to create the mesh of the open subset Ω , we are going to depend on the image pixels as a step, that means we will work locally for each pixel in the digital image.
For time step τ, we depend on the image clarification sought in image acquisition process where

$$\tau = \frac{T}{N'}$$

T is the time range, N' is the number of iterance and $\tau = 1...T$ time index. The open subset $\Omega = (a, b) \times (a\prime, b\prime)$ becomes $\Omega = [M, N]$ and the digital image I becomes discrete one.

$$I(t, x, y) = I(k, i, j) = I^k_{ij}.$$

Where $[M, N]$ is the image size and (i, j) pixel coordinates with M is the number of image lines, $i = 1...M$ image pixel line, N is the number of image columns, $j = 1...N$ image pixel column. Using Euler explicit scheme to discretize the mathematical system (1.1) above, equations$(2.1) - (2.6)$ are approximated equations applied into the proposed system terms $(3.1) - (3.4)$ to reach their discretization.

1: The diffusion problem coefficient term stills the same

$$c(t) = 1 + \frac{1}{\sqrt{4+t^2}}. \tag{3.1}$$

2: The convolution product,we apply Simpsons improved method

$$(\nabla G_\sigma * I)(x, y) = \int_\Omega \int_\Omega \nabla G_\sigma(x - \tau_1, y - \tau_2).I(\tau_1, \tau_2) d\tau_2 d\tau_1.$$

For $\Omega = (a, b) \times (a', b')$ $\forall (x, y) \in \Omega$; in order to, we subdivide Ω

-: $h_1 = \frac{b-a}{M}$, $x_m = a + mh_1$ for $x \in (a, b)$ and $m = 1...M$.

-: $h_2 = \frac{b'-a'}{N}$, $y_n = a + nh_2$ for $y \in (a', b')$ and $n = 1...N$.

With Simpsons improved method, the integral approximation is

$$\int_{x_{m-1}}^{x_{m+1}} f(t)dt \simeq \frac{h}{3}\left[f\left(x_{m-1}\right)+4f\left(x_{m}\right)+f\left(x_{m+1}\right)\right].$$

That gives us the convolution product as

$$\begin{aligned}
&\left(\nabla G_{\sigma} * I\right)(x,y) = \sum_{m=1}^{M-1}\sum_{n=1}^{N-1}\int_{x_{m-1}}^{x_{m+1}}\int_{y_{n-1}}^{y_{n+1}}\left[\nabla G_{\sigma}(x-\tau_1, y-\tau_2).I(\tau_1,\tau_2)d\tau_2 d\tau_1\right]\\
&\simeq \sum_{m=1}^{M-1}\sum_{n=1}^{N-1}\tfrac{h_1 h_2}{9}\left[\nabla G_{\sigma}(x_{m-1},y_{n-1}).I(x_{m-1},y_{n-1})\right.\\
&+4.\nabla G_{\sigma}(x_m,y_{n-1}).I(x_m,y_{n-1})+\nabla G_{\sigma}(x_{m+1},y_{n-1}).I(x_{m+1},y_{n-1})\\
&+4.\nabla G_{\sigma}(x_{m-1},y_n).I(x_{m-1},y_n)+16.\nabla G_{\sigma}(x_m,y_n).I(x_m,y_n)\\
&+4.\nabla G_{\sigma}(x_{m+1},y_n).I(x_{m+1},y_n)+\nabla G_{\sigma}(x_{m-1},y_{n+1}).I(x_{m-1},y_{n+1})\\
&\left.+4.\nabla G_{\sigma}(x_m,y_{n+1}).I(x_m,y_{n+1})+\nabla G_{\sigma}(x_{m+1},y_{n+1}).I(x_{m+1},y_{n+1})\right]
\end{aligned} \qquad (2.1).$$

3: Since we already considered the digital image as discrete one where $h_1{=}h_2$ = pixel and we have G_σ Gauss kernel for sets with dimension ($dim = 2$) calculated as

$$G_{\sigma}(x,y) = \frac{1}{2.\pi.\sigma^2}\exp\left(-\frac{x+y}{2.\sigma^2}\right).$$

Then its gradient ∇G_σ applied for discrete imaeg is

$$\nabla G_{\sigma}(x,y) = \nabla G_{\sigma ij} = \begin{pmatrix} \frac{-i}{2.\pi.\sigma^4}\exp\left(-\frac{i+j}{2.\sigma^2}\right) \\ \frac{-j}{2.\pi.\sigma^4}\exp\left(-\frac{i+j}{2.\sigma^2}\right) \end{pmatrix}.$$

We obtain

$$\begin{aligned}
&\left|\nabla G_{\sigma} * I\right|(i,j) = \left|\tfrac{1}{9}\sum_{m=1}^{M-1}\sum_{n=1}^{N-1}\right.\left[\nabla G_{\sigma}(i-1,j-1).I(i-1,j-1)\right.\\
&+4.\nabla G_{\sigma}(i,j-1).I(i,j-1)+\nabla G_{\sigma}(i+1,j-1).I(i+1,j-1)\\
&+4.\nabla G_{\sigma}(i-1,j).I(i-1,j)+16.\nabla G_{\sigma}(i,j).I(i,j)\\
&+4.\nabla G_{\sigma}(i+1,j).I(i+1,j)+\nabla G_{\sigma}(i-1,j+1).I(i-1,j+1)\\
&+4.\nabla G_{\sigma}(i,j+1).I(i,j+1)+\nabla G_{\sigma}(i+1,j+1).I(i+1,j+1)\\
&+4.\nabla G_{\sigma}(i,j+1).I(i,j+1)+\nabla G_{\sigma}(i+1,j+1).I(i+1,j+1)\\
&\left.+4.\nabla G_{\sigma}(i,j+1).I(i,j+1)+\nabla G_{\sigma}(i+1,j+1).I(i+1,j+1)\right|.
\end{aligned} \qquad (3.2)$$

4: The degenerated diffusion term includes multi factors and operators to deal with, we apply Taylor method for first and second derivatives approximation and the gradient norm $|\nabla I|$ is the second norm.

Theorem 2.1. *Tylor method for approximation*
if f is n-differentiable function from a set E into a set F and $n \geq 2$,

$$\forall x \in E : f(x) = \sum_{k=0}^{n}\frac{f^{(k)}(a)}{k!}(x-a)^k + R_n(x) \quad R_n(x) \underset{x\longrightarrow a}{\longrightarrow} 0 \quad a \in E$$

- $I_t = \frac{\partial I}{\partial t}(t,x,y)$ is the first derivative of the function I for time τ and its approximation
$$I_t \simeq \tfrac{I(t+1,x,y)-I(t,x,y)}{\tau} + O(\tau) \qquad \begin{smallmatrix} O(\tau)\longrightarrow 0 \\ \tau\longrightarrow 0 \end{smallmatrix}.$$
For discretization we get
$$I_\tau = \frac{I_{ij}^{k+1} - I_{ij}^k}{\tau}. \tag{2.2}$$
- $I_x = \frac{\partial I}{\partial x}(t,x,y)$ is the first derivative of the function I for x and its approximation.
$$I_x \simeq \tfrac{I(t,x+1,y)-I(t,x,y)}{h_1} + O(x) \qquad \begin{smallmatrix} O(x)\longrightarrow 0 \\ x\longrightarrow 0 \end{smallmatrix}.$$
For discretization we get
$$I_x = \frac{I_{i+1j}^k - I_{ij}^k}{h_1}$$
- $I_y = \frac{\partial I}{\partial y}(t,x,y)$ is the first derivative of the function I for y and its approximation
$$I_y \simeq \tfrac{I(t,x,y+1)-I(t,x,y)}{h_2} + O(x) \qquad \begin{smallmatrix} O(y)\longrightarrow 0 \\ y\longrightarrow 0 \end{smallmatrix}.$$
For discretization we get
$$I_y = \frac{I_{ij+1}^k - I_{ij}^k}{h_2}$$
so, with $h_1 = h_2 = pixel$, we arrive to
$$I_x = I_{i+1j}^k - I_{ij}^k \tag{2.3}$$
$$I_y = I_{ij+1}^k - I_{ij}^k. \tag{2.4}$$

Used in the second norm for the gradient $|\nabla I| = \begin{vmatrix} I_x \\ I_y \end{vmatrix}$, we obtain
$$|\nabla I| = \begin{vmatrix} I_x \\ I_y \end{vmatrix} = \sqrt{\left(I_{i+1j}^k - I_{ij}^k\right)^2 + \left(I_{ij+1}^k - I_{ij}^k\right)^2}. \tag{3.3}$$

- For the L^1 operator $div\left(\frac{\nabla I}{|\nabla I|}\right)$.
- $I_{xx} = \frac{\partial^2 I}{\partial x^2}(t,x,y)$ is the second derivative of the function I for $x$and its approximation
$$I_{xx} = I_{i+1j}^k - 2.I_{ij}^k + I_{i-1j}^k. \tag{2.5}$$
- $I_{yy} = \frac{\partial^2 I}{\partial y^2}(t,x,y)$ is the second derivative of function I for y and its approximation
$$I_{yy} = I_{ij+1}^k - 2.I_{ij}^k + I_{ij-1}^k. \tag{2.6}$$

Then the divergent will be

$$div\left(\frac{\nabla I}{|\nabla I|}\right)=\frac{I_i^2.I_{jj}+I_j^2 I_{ii}-2.I_i I_j I_{ij}}{\left(I_i^2+I_j^2\right)^{\frac{3}{2}}}. \tag{3.4}$$

Finally, the equations (3.1), (3.2), (3.3) and (3.4) give the approximation of the problem (1.1).

2.2. **Problem stability.**

Theorem 2.2. *Let the problem $L.U=f$*
with L : differential operator, U, f : differential function ;
where its perturbed one is $L.U^{(h)}=f^{(h)}$.
Euler explicit scheme of the problem $L.U=f$ is stable if :

$\exists\delta>0$, $\exists h_0>0$ $\forall h_0<h_0$, $\forall\delta f^{(h)}\in F_h$, such as , $L.U^{(h)}=f^{(h)}+\delta f^{(h)}$ accepts unique solution $Z^{(h)}\in U_0$, further more , $\left\|Z^h-U^h\right\|_{U_h}\leq\alpha\left\|f^h\right\|_{F_h}$

$Z^{(h)}$ is the approximated solution $U^{(h)}$ is the approximated solution space.
$f^{(h)}$ is the approximated fuction $F^{(h)}$ is the approximated function space.

We apply the previous theorem on our problem (1.1), when the subset Ω is associated with the norm sup.
In $I_t=\frac{\partial I}{\partial t}$, the operator $\frac{\partial .}{\partial .}$ is linear so, we prove that

$$\left\|I^{(h)}\right\|_{\Omega_h}\leq\alpha\left\|f^{(h)}\right\|_{\Omega_h}$$

where I is the image and $f(t,x,y)=c(t).\left|\nabla G_\sigma * I\right|.\left|\nabla I\right|.div\left(\frac{\nabla I}{|\nabla I|}\right)$. We have for the first equation in system (1.1)

$$I_t=\frac{I(t+1,x,y)-I(t,x,y)}{\tau}\quad\text{and}\quad I_t=f(k,i,j)$$

we have

$$\frac{I(k+1,i,j)-I(k,i,j)}{\tau}=f(k,i,j)$$

than we have

$$\begin{gathered}I(k+1,i,j)=I(k,i,j)+\tau.f(k,i,j)\\ \left|I_{ij}^{k+1}\right|=\left|I_{ij}^k+\tau.f_{ij}^k\right|\\ \max_{i,j}\left|I_{ij}^k\right|\leq\ \max_{i,j}\left|I_{ij}^{k-1}\right|+\tau.\max_{i,j}\left|f_{ij}^k\right|\\ .\\ .\\ \max_{i,j}\left|I_{ij}^1\right|\leq\ \max_{i,j}\left|I_{ij}^0\right|+\tau.\max_{i,j}\left|f_{ij}^k\right|.\end{gathered}$$

By addition side by side and same terms reduction, we get

$$\begin{gathered}\max_{i,j}\left|I_{ij}^k\right|\leq\ \max_{i,j}\left|I_{ij}^0\right|+n.\tau.\max_{i,j}\left|f_{ij}^k\right|\\ \left\|I^{(h)}\right\|_{\Omega_h}\leq\alpha\left\|f^{(h)}\right\|_{\Omega_h}\end{gathered}$$

such as $T=n.\tau$ so the schema is stable for $\alpha=1+T$.

3. Experimental results

In order to estimate the efficiency of our image enhacement and restoration model, we carry out the algorithm and simulation using a Windows PC in system powered by Intel 2.6 GHz and 64 bit operating system with 4GB RAM. The experiments are performed using MATLAB R2017a software[14] on different types of noise, take advantage from the image processing toolbox and adjudicating to **PSNR**, **RMSE** and **SSIM**; with time interval took between $\tau = 1s$ to $\tau = 60s$ according to noise type and number for iterations, noting that

MSE: Mean Square Error is the cumulative squared error between the original and the noised image.

RMSE: Root of Mean Square Error.

PSNR: Peak Signal to Noise Ratio gives a noise free monochrome for image and its noisy approximation.

SSIM: Structure Similarity Index Metrix is a method for predicting the perceived quality of measuring the similarity between two images, usually original image and restored image.

$$\mathbf{MSE}(I) = \frac{1}{mn} \sum_{i=0}^{m-1} \sum_{j=0}^{n-1} \left[I(i,j) - I'(i,j) \right]^2$$

with (m, n) is the image size; $I^{'}$ restored image and I original image.

$$\mathbf{RMSE} = \sqrt{\mathbf{MSE}(I)}$$

$$\mathbf{PSNR} = 10.\log_{10} \left(\frac{255^2}{\mathbf{MSE}} \right)$$

$$\mathbf{SSIM} = \frac{(2\mu_i\mu_j + c_1)(2\sigma_{ij} + c_2)}{\left(\mu_i^2 + \mu_j^2 + c_1\right)\left(\sigma_i^2 + \sigma_j^2 + c_2\right)} \text{ with}$$

μ_i is the average of x pixels; μ_j is the average of y pixels;
σ_i^2 is the variance of x pixels; σ_j^2 is the variance of y pixels;
and σ_{ij} is the covariance of x pixels and y pixels.
$c_1 = (0.01 \cdot L)^2$ and $c_2 = (0.03 \cdot L)^2$ are two variables to stabilize the division with weak denominator, L is the dynamic range of the pixel values (typically this is 255).

The noised image restoration and the manipulation of the algorithm concluded by programming the Euler explicit scheme for discretization of proposed system are done in MATLAB R2017a into the following steps: **Step 1**: program the convolution product based on the Gaussian kernel as mask with σ standard deviation and scale parameter.

Step 2: verify the image dimension that should be $dim = 2$ then convert the image in gray level with single values for pixels.

Step 3: filter the image by motion by mean curvature in to detect degraded pixels.

Step 4: determine time step by $\tau = 1s$ and the number of iterations K and σ standard deviation for filtring Gaussian noise.

Step 5: start a loop from $l = 1$ to $l = K$ restoring degraded pixels and enhance image, calculating **RMSE**, **PSNR** and **SSIM** for better result we achieve.

The first table shows noised image manipulation to rid of salt and pepper noise after $K = 4$ iterations and time step estimate to $\tau = 1s$. The second table shows noised image manipulation to rid of additive Gaussian noise, this time after $K = 40$ iterations but the same time step estimates to $\tau = 1s$.

Original Image	**Noised Image**	**Restored Image**	**PSNR**	**Our Proposed Approach**	
				Restored Image	**PSNR**
			24.49		24.63
			19.64		20.03
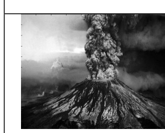	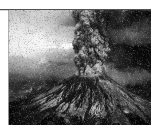		34.85	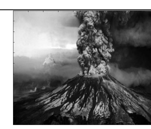	35.06
	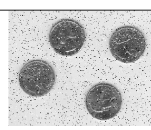		27.43		27.62

TABLE 1. Salt and Pepper noise d = 0.05 K = 4.

Original Image	**Noised Image**	**Restored Image** (Weiner Filter)	PSNR	SSIM	**Our Proposed Approach**		
					Restored Image	PSNR	**SSIM**
	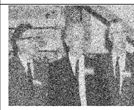	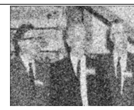	27.53	0.27		33.13	0.17
			33.03	0.12		31.86	0.16
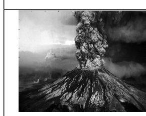		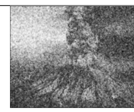	31.61	0.20	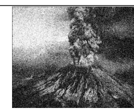	34.44	0.11
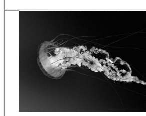	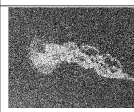	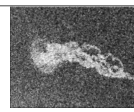	31.52	0.11	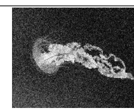	35.84	0.07
	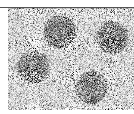	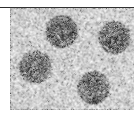	30.67	0.07	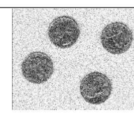	29.98	0.10

TABLE 2. Additive Gaussaian noise $\sigma = 0.05$ K = 4.

4. Comparison with other approaches

4.1. **Approaches based on anisotropic diffusion model.** S. A. Halim, and N. N. Wira [8] propose two diffusion functions which known as diffusion function 1 ($DF-1$) and diffusion function 2 ($DF-2$) by the following forms

$$DF-1: \ \delta_{u\ 1}(s) = \frac{1}{1+\left(\frac{s+s\sqrt{255}}{K}\right)^2}$$

$$DF-2: \ \delta_{u\ 2u\ 1}(s) = e^{\left(-\left(\frac{s+s\sqrt{5}}{K}\right)^2\right)}$$

where s is image gradient and K is a threshold to control the diffusion process.

DF-1 follows the properties of the diffusion function as when s approaches ∞, it tends to become 0 and when s approaches 0, the value is 1. Meanwhile, DF-2 was proposed by modifying and enhancing the diffusion function proposed by Tsiotsios and Petrou since the diffusion function preserves the edges better in the images.

In the proposed approach by E. Cuevas and al. [5] , the appropriate anisotropic diffusion parameter values for filtering the noised images are obtained as the solution that involves the best possible trade-off between two conflicting objective functions. The optimization process considers the minimization of the noise contained in the image, while the contrast of the main characteristics of the original image is maximized.

R. R .Nair and al.[12] propose a methodology based on the concept that the immediate future value of the intensity of a candidate pixel can be predicted in terms of the estimate of the increment or decrement of the pixel intensity in terms of the directional derivatives with respect to neighborhood pixels inside an open subset. The prediction equation is a novel mathematical model developed from Einstein's stochastic argument for Brownian motion.

Whilst A.Theljani and al. in [16] consider a non standard high-order nonlinear diffusion equation in analogy with the Total Variation and biharmonic models, the high-order diffusion models perform better than second-order ones in image denoising for edge and curvature preserving issues In fact, they are able to reproduce features of "high-order" (curvature, corners, etc.) and allow the matching of edges across large distances due to the supplementary information provided by high-order derivatives, whereas in the homogeneous zones they enforce the smoothing effect.

In the same approach, a qualitative analysis and numerical simulations of a nonlinear second-order anisotropic diffusion problem with non-homogeneous Cauchy–Neumann boundary conditions presented by T. Barbu and al. in [2].

Also, for the two phase ultrasound Image de-speckling Framework by nonlocal means on anisotropic diffused image data a qualitative analysis and numerical simulations of a nonlinear second-order anisotropic diffusion problem with non-homogeneous Cauchy-Neumann boundary conditions [15].

Compared Approach	Original Image	Noised Image	Restored Image	PSNR	Our Proposed Approach	
					Restored Image	SSIM
[8]		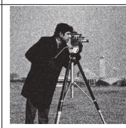		24.49		0.7931
[5]	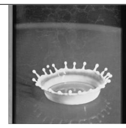	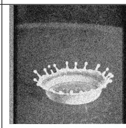	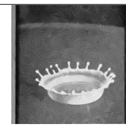	19.64	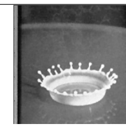	0.8025
[12]				34.85		0.5177
[2]	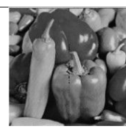		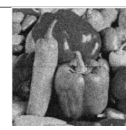	27.43	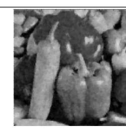	0.7026
[15]	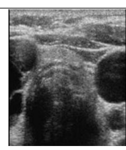		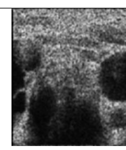	19.40	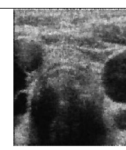	0.7089

Table 3. Comparing with Anisotropic diffusion approaches results.

For restoration method mentioned in [16], the original image isn't available, hence we calculate SSIM instead of PSNR between their and our restored images in table.4.

Compared Approach	Original Image	Noised Image	Restored Image	PSNR	Our Proposed Approach	
					Restored Image	SSIM
[16]	**Not available**	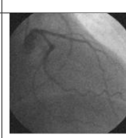	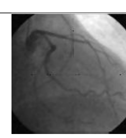	32.01		0.8462

Table 4. Comparing with Anisotropic diffution approaches results.

4.2. **Approches based on various other methods.** Image processing is an expanding field of researches, we are going to compare **PSNR** of results obtained through image manipulation by other methods than Anisotropic Diffusion ones and results generated by our proposed model.
A. Lanza and al. in [10] focus on the choice of the sparsity-promoting regularizer and propose the parameterized non convex non separable regularizer

$$R_B(x) := R(x) - \left(R \,\square \frac{1}{2} \|B.\|_2^2\right)(x).$$

Where $\square$ denotes the infimal convolution operator and matrix $B \in \mathbb{R}_{q\times n}$ is a parameter.
J. Xu and al.[17] present a novel variational model for image decomposition by proposed system contains two variational minimization problems: one is a high-order variational problem with L^2 norm for the data fidelity term, while the other includes a Tikhonov regularization for one introduced vector and bring in an auxiliary variable to split **LLT** model.
Based on keeping the useful multiorder structure information from lost, H. Zeng and al.[18] generalize the denoising algorithm for 2- order tensors case to 3-order tensors by solving the problem

$$\begin{aligned} &\arg\min_{\mathcal{L}} \;\; rank(\mathcal{L}) + \lambda \|S\|_0 \\ &s.t \;\; \mathcal{O} = \mathcal{L} + \mathcal{S} + \mathcal{N} \end{aligned}$$

where $\mathcal{O}$; $\mathcal{L}$; $\mathcal{S}$ and $\mathcal{N} \in \mathbb{R}^{m\times n\times p}$; $\mathcal{O}$ denotes the observed hyperspectral image; $\mathcal{L}$ represents the clean hyperspectral image data; $\mathcal{S}$ is the sparse noise which consists of impulse noise, stripes, deadline and so on; $\mathcal{N}$ is the Gaussian noise; $m \times n$ is the spatial size of the hyperspectral image, and p is the number of spectral bands.

Compared Approach	Original Image	Noised Image	Restored Image	PSNR	Our Proposed Approach	
					Restored Image	SSIM
[10]		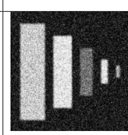	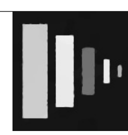	22.92	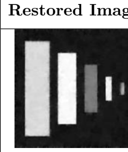	0.8314
[17]	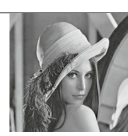		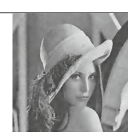	29.55		0.7438
[18]				37.15		0.7635

Table 5. Comparing with various approaches results.

5. Conclusion

Even with the growth and the increase of algorithms and academic researchs in the image restoration and denoising field, based on varied mathematical models perturbation, PDE in Anisotropic Diffusion remains more lean on for image restoration as a result of its robust handling the image properties by smoothing with edge preservation and treating each pixel locally and their algorithms exhibit better, so our proposed model even simple but involves powerful terms with efficient performance as concludes higher results estimated to 7% as seen in the tables1, 2, 3 and 4 present a link with good approaches for those kind of noise.

6. Acknowledgments

The author wish to thank the referee for the helpful suggestions and comments.

References

1. L. Alvarez, PL. Lions, JM. Morel, Image Selective Smoothing and Edge Detection by Nonlinear Diffusion, *SIAM J. NUMER*, **29**(3), (1992), 845-866.
2. T. Barbu, A. Miranville, C. Moro, A Qualitative Analysis and Numerical Simulations of a Nonlinear Second-order Anisotropic Diffusion Problem with Non-homogeneous Cauchy–Neumann Boundary Conditions, *Applied Mathematics and Computation*, **350**, (2019), 170-180.
3. A. Boucher, *Image Processing-spatial Convolution-*, www.etud.iro, 2016.
4. V. Choqueuse, *Convolution Product-principe and Propieties*, Westerner Britann, 2016.
5. E. Cuervas, H. Becerra, A. Luque, Anisotropic Diffusion Filtering Through Multi-objective Optimization, *Mathematics and Computers in Simulation*, **181**, (2020), 410-429.
6. M. Gatcha, F. Messelmi, S. Saadi, An Anisotropic Diffusion Adaptive Filter for Image Denoising and Restoration Applied on Satellite Remote Sensing Images: a Case Study, *Engineering Technology & Applied Science Research*, **12**(6), (2022), 9715-9719.
7. S. Godounov, V. Riabenki, *Differences Schemes (Introduction of the Theory)*, University publication office, Algeria, 1987.
8. S. A. Halim, N. N. Wira, Variations of Diffusion Functions on Perona and Malik Model for Noise Removal, Fourth-order Partial Differ, *AIP Conference Proceedings*, **2266**(1), (2020), 1-8.
9. J. J. Koenderink, The Structure of Images, *Biological Cybernetics*, **50**, (1984), 363-370.
10. A. Lanza, S. Morigi, IW. Selesnick, F. Sgallari, Sparsity-inducing Nonconvex Non Separable Regularization for Convex Image, *Society for Industrial and Applied Mathematics*, **12**(2), (2019), 1099-1134.
11. D. Marr, E. Hildreth, Theory of Edge detection, *Proceedings of the Royal Society Series B Biological Sciences*, **207**(1167), (1980), 187-217.
12. R. R. Nair, E. David, S. Rajagopal, A Robust Anisotropic Diffusion Filter with Low Arithmetic Complexity for Images, *EURASIP Journal on Image and Video Processing*, **48**, (2019).
13. P. Perona, J. Malik, Scale-space and Edge Detection Using Anisotropic Diffusion, *IEEE Transactions On Pattern Analysis And Machine Intelligence*, **12**(7), (1990), 629-639.

14. J. C. Russ,*The Image Processing Cookbook*, 4th edition, USA, 2017.
15. N. Thakur, N. U. Khan, S. D. Sharma, A Two Phase Ultrasound Image De-speckling Framework by Nonlocal Means on Anisotropic Diffused Image Data, *Informatica*, **47**(2), (2023), 221-234.
16. A. Theljani, Z. Belhachmi, M. Moakher, High-order Anisotropic Diffusion Operators in Spaces of Variable Exponents and Application to Image Inpainting and Restoration Problems, *Nonlinear Analysis Real World Applications*, **47**, (2019), 251-271.
17. J. Xu, Y. Hao, M. Li, X. Zhang, A Novel Variational Model for Image Decomposition, *Signal and Image and Video Processing*, **13**, (2019), 967–974.
18. H. Zeng, X. Xie, J. Ning, Hyperspectral Image Denoising via Global Spatial-spectral Total Variation Regularized Nonconvex Local Low-rank Tensor Approximation, *Signal Processing*, **178**, (2021).